Electronic Supplementary Information

Configurational and energetical study of the (100) and (110) surfaces of the $MgAl_2O_4$ spinel by means of quantum-mechanical and empirical techniques

Francesco Roberto Massaro,[1] Marco Bruno,[2] Fabrizio Nestola[1]

[1]Dipartimento di Geoscienze – Università di Padova, via G. Gradenigo 6, I-35131 Padova, Italy

[2]Dipartimento di Scienze della Terra - Università di Torino, via Valperga Caluso 35, I-10125 Torino, Italy.

(100) configurations

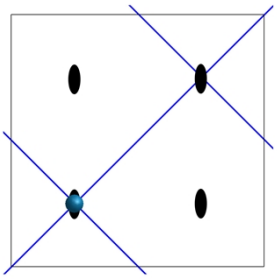

cut1

Figure S1. The (100) cell configuration of the *cut1*. Blue is for Mg ion. The symmetry elements (the two-fold axes and the *m* planes) are reported as well.

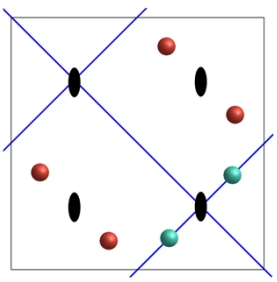

***cut2*α_1**

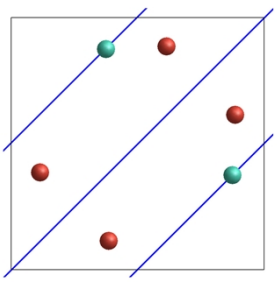

***cut2*α_2**

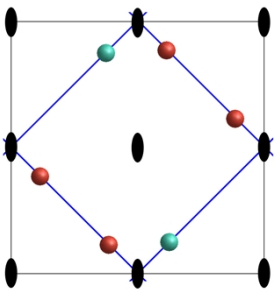

***cut2*α_3**

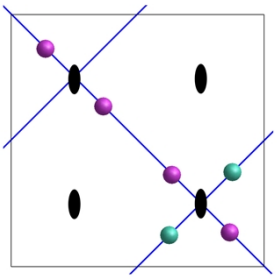

$cut2\beta_1$

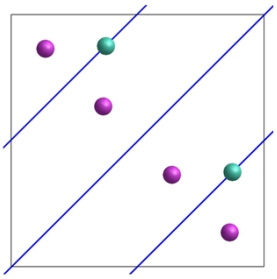

$cut2\beta_2$

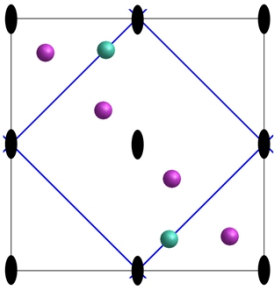

$cut2\beta_3$

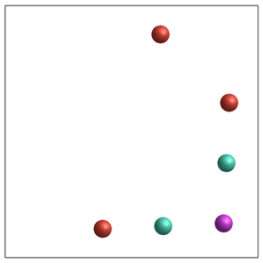

$cut2\gamma_{a1}$

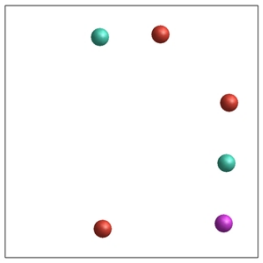

$cut2\gamma_{a2}$

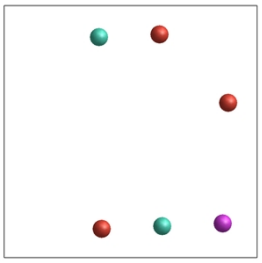

$cut2\gamma_{a3}$

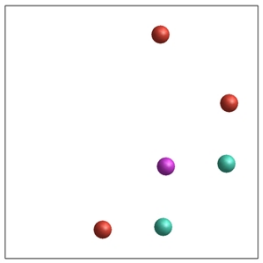

$cut2\gamma_{b1}$

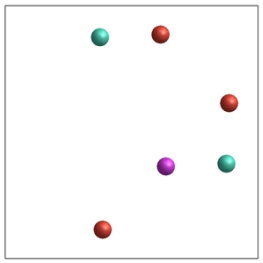

$cut2\gamma_{b2}$

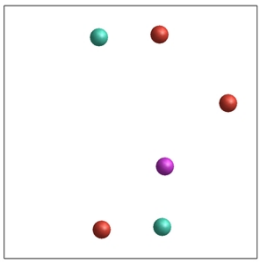

$cut2\gamma_{b3}$

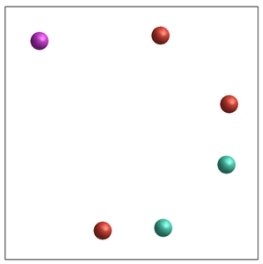

$cut2\gamma_{c1}$

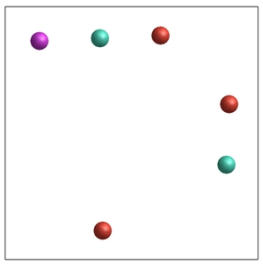

$cut2\gamma_{c2}$

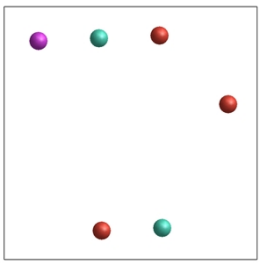

$cut2\gamma_{c3}$

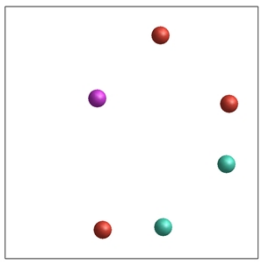

$cut2\gamma_{d1}$

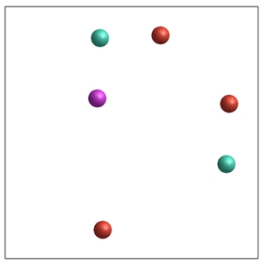

$cut2\gamma_{d2}$

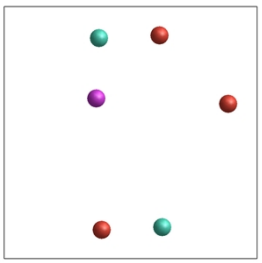

$cut2\gamma_{d3}$

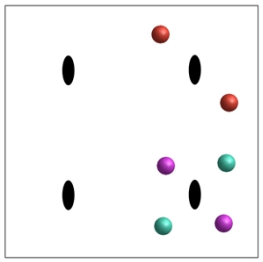

$cut2\delta_{a1}$

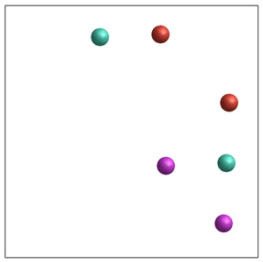

$cut2\delta_{a2}$

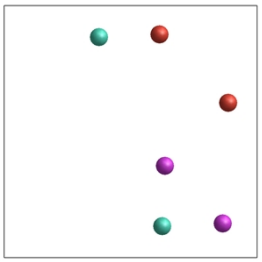

$cut2\delta_{a3}$

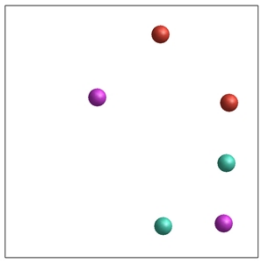

$cut2\delta_{b1}$

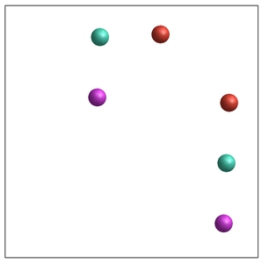

$cut2\delta_{b2}$

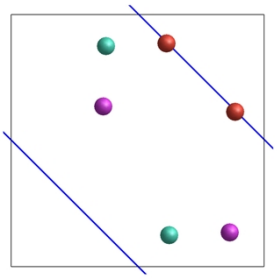

$cut2\delta_{b3}$

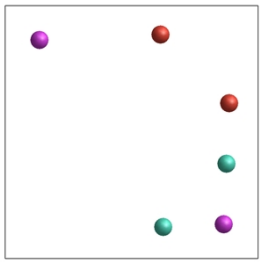

$cut2\delta_{c1}$

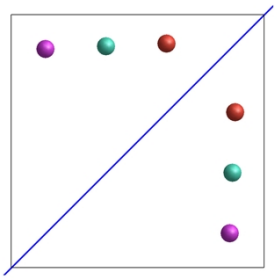

$cut2\delta_{c2}$

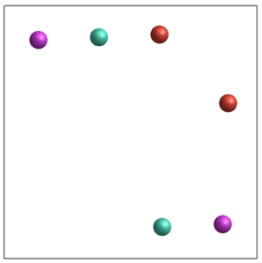

$cut2\delta_{c3}$

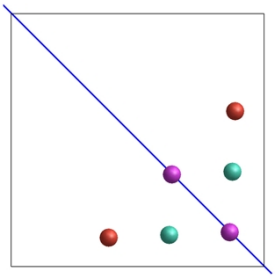

$cut2\delta_{d1}$

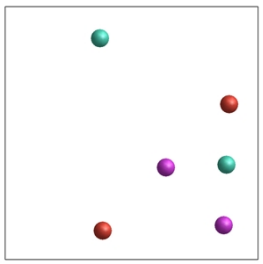

$cut2\delta_{d2}$

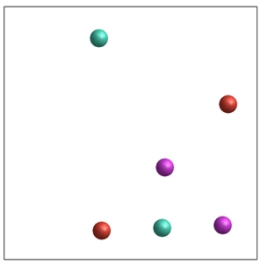

$cut2\delta_{d3}$

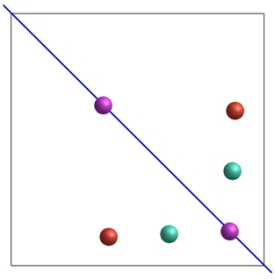

$cut2\delta_{e1}$

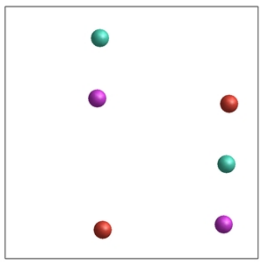

$cut2\delta_{e2}$

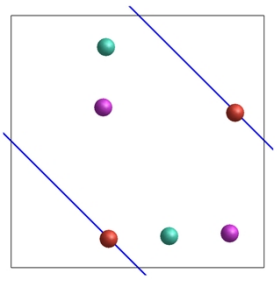

$cut2\delta_{e3}$

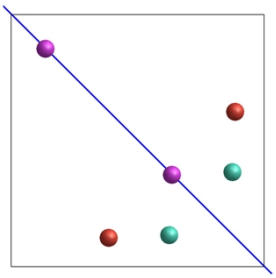

cut2δ_{f1}

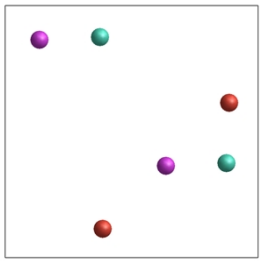

cut2δ_{f2}

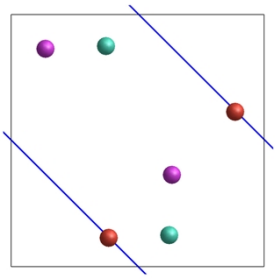

cut2δ_{f3}

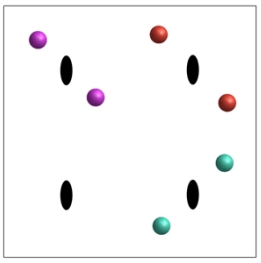

cut2δ_{q1}

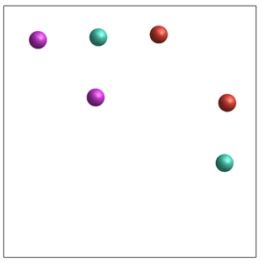

cut2δ_{q2}

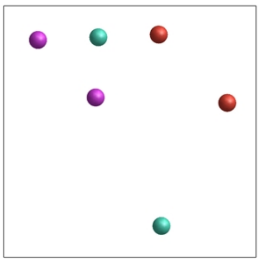

cut2δ_{q3}

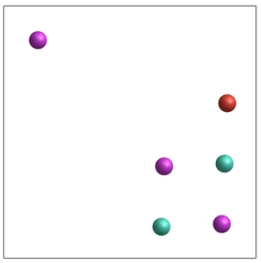

cut2ε_{a1}

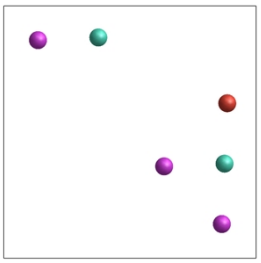

cut2ε_{a2}

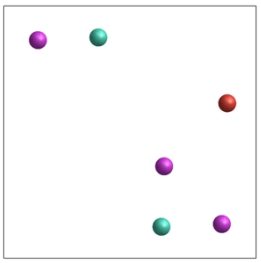

cut2ε_{a3}

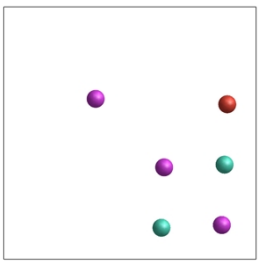

cut2ε_{b1}

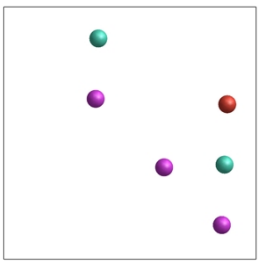

cut2ε_{b2}

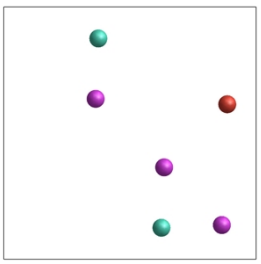

cut2ε_{b3}

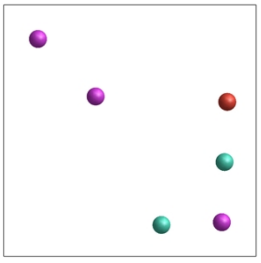

cut2ε_{c1}

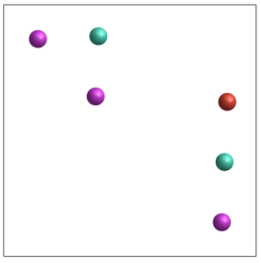

cut2ε_{c2}

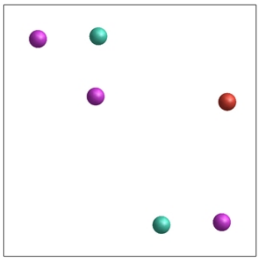

cut2ε_{c3}

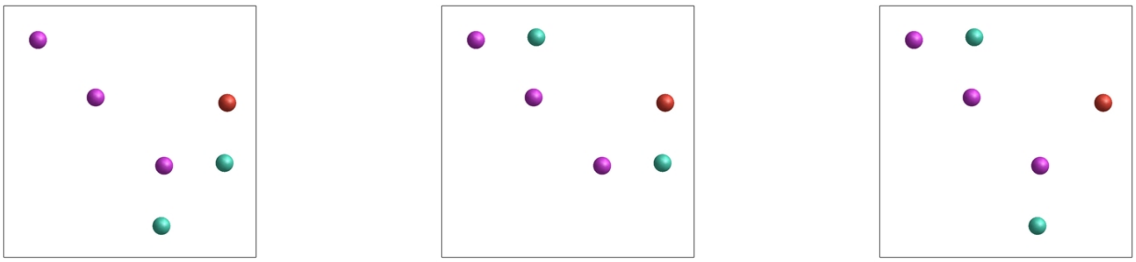

Figure S2. The fifty-one (100) cell configurations of the *cut2*. The colors stand: red for the O bonded to Mg (O1), purple for the O bonded only to Al (O2) and greenish for the Al. The symmetry elements (the two-fold axes and the *m* planes) are reported as well.

(110) configurations

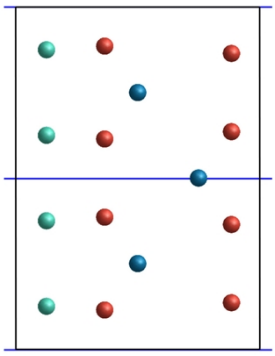

cut1

Figure S3. The (110) cell configuration of the *cut1*. The colors stand: red for the O bonded to Mg (O1), purple for the O bonded only to Al (O2), greenish for the Al and blue for the Mg ions. The *m* plane is reported as well.

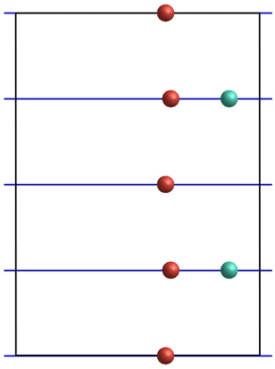

cut2α_1

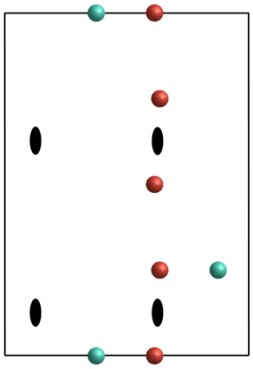

cut2α_2

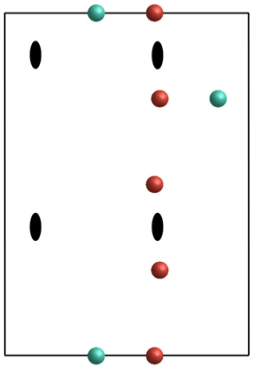

cut2α_3

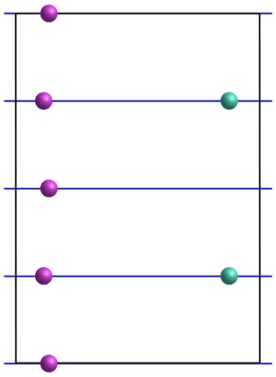

cut2β_1

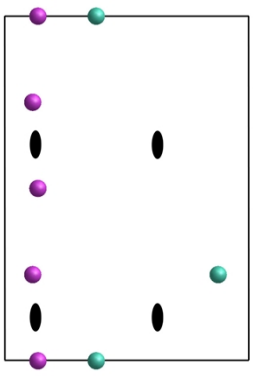

cut2β_2

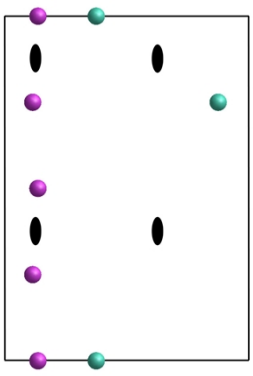

cut2β_3

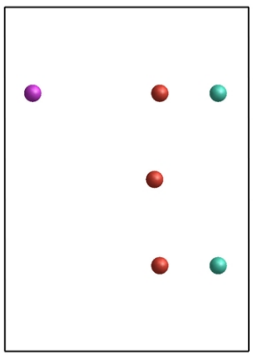

$cut2\gamma_{a1}$

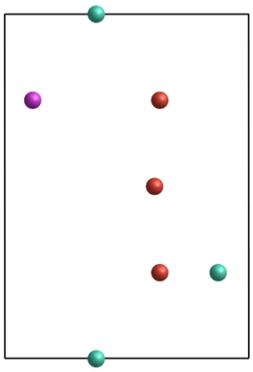

$cut2\gamma_{a2}$

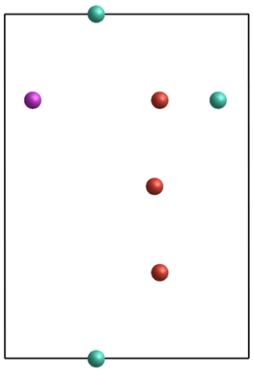

$cut2\gamma_{a3}$

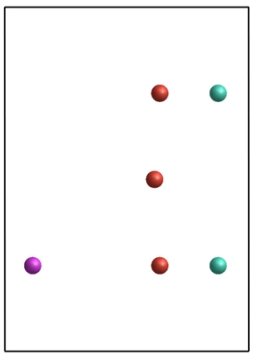

$cut2\gamma_{b1}$

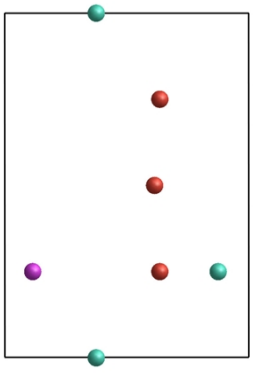

$cut2\gamma_{b2}$

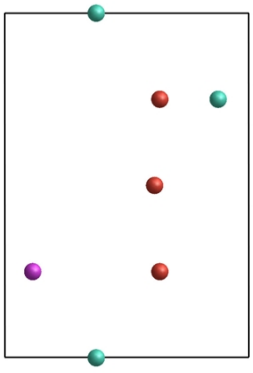

$cut2\gamma_{b3}$

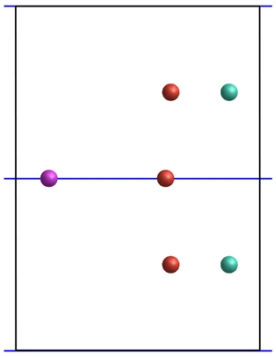

$cut2\gamma_{c1}$

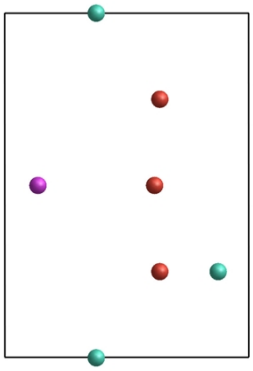

$cut2\gamma_{c2}$

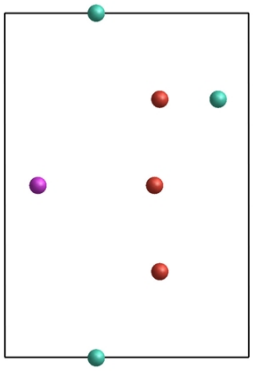

$cut2\gamma_{c3}$

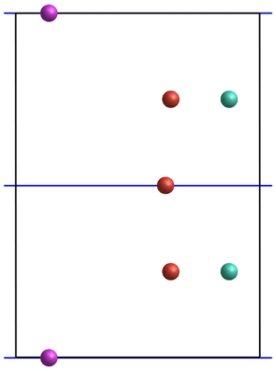

$cut2\gamma_{d1}$

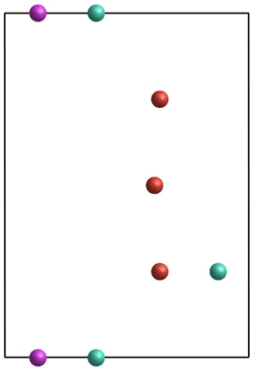

$cut2\gamma_{d2}$

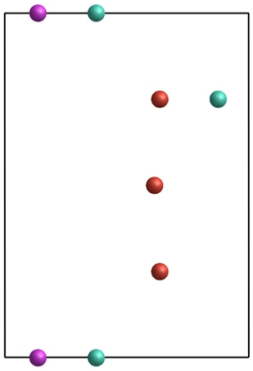

$cut2\gamma_{d3}$

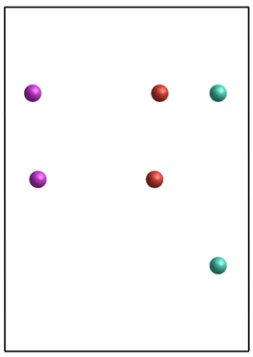

$cut2\delta_{a1}$

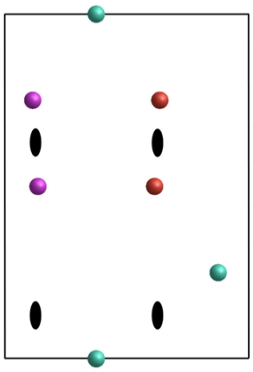

$cut2\delta_{a2}$

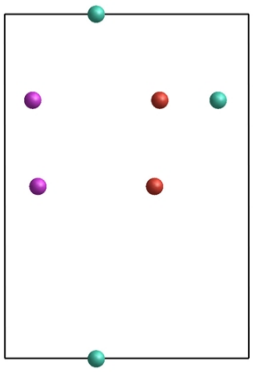

$cut2\delta_{a3}$

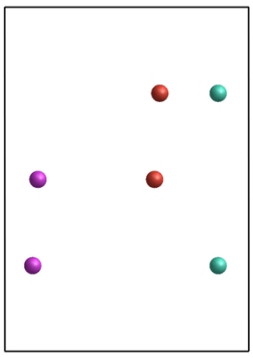

$cut2\delta_{b1}$

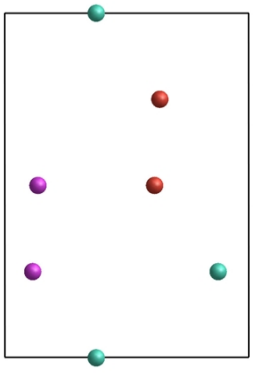

$cut2\delta_{b2}$

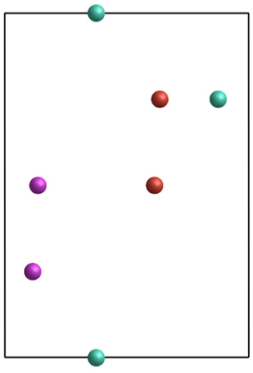

$cut2\delta_{b3}$

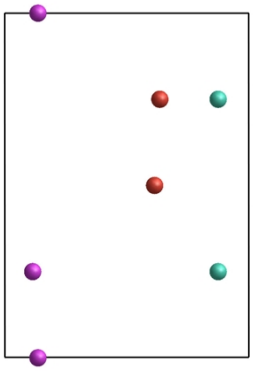

$cut2\delta_{c1}$

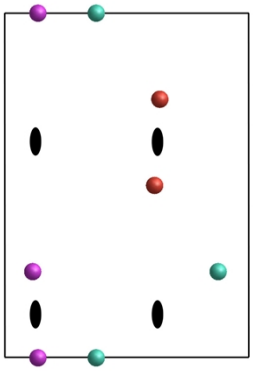

$cut2\delta_{c2}$

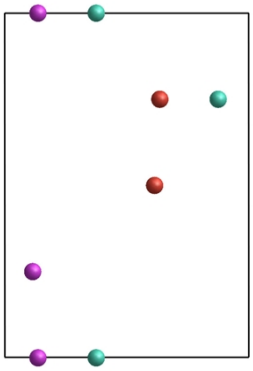

$cut2\delta_{c3}$

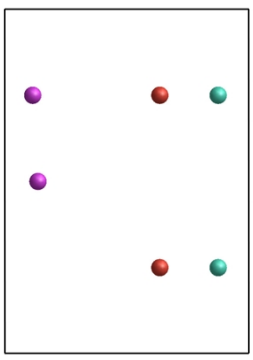

$cut2\delta_{d1}$

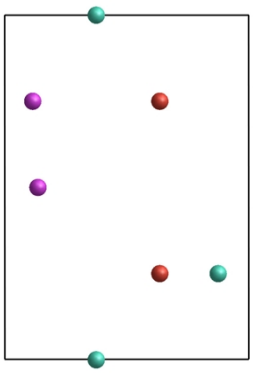

$cut2\delta_{d2}$

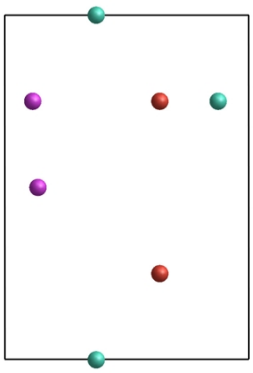

$cut2\delta_{d3}$

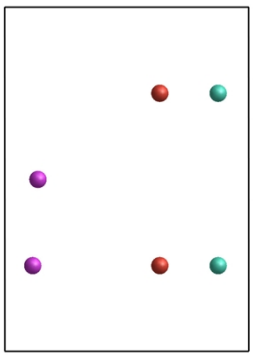

$cut2\delta_{e1}$

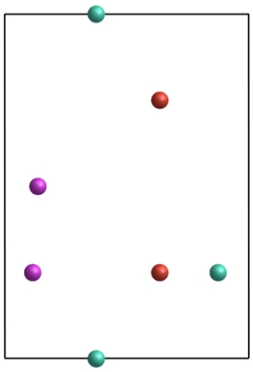

$cut2\delta_{e2}$

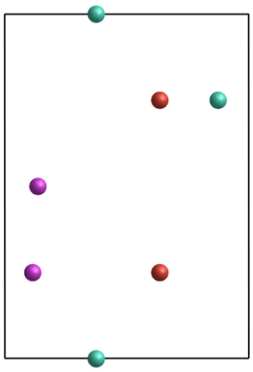

$cut2\delta_{e3}$

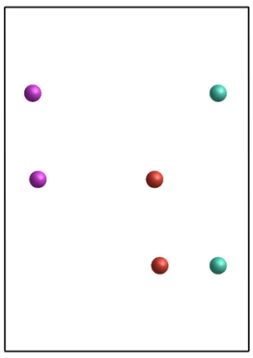

$cut2\delta_{f1}$

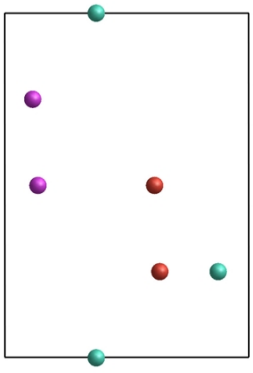

$cut2\delta_{f2}$

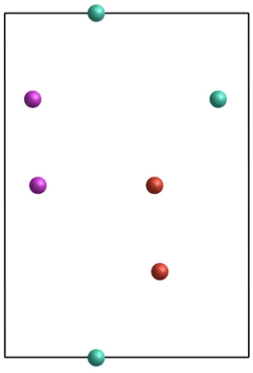

$cut2\delta_{f3}$

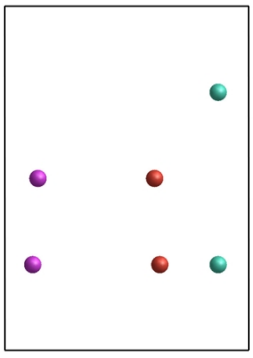

$cut2\delta_{g1}$

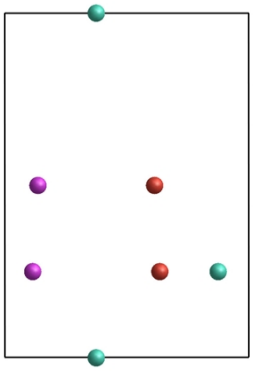

$cut2\delta_{g2}$

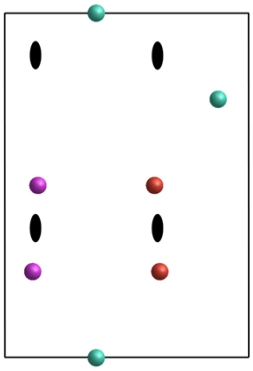

$cut2\delta_{g3}$

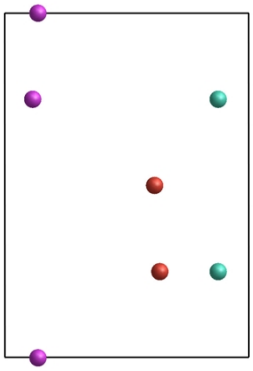

$cut2\delta_{h1}$

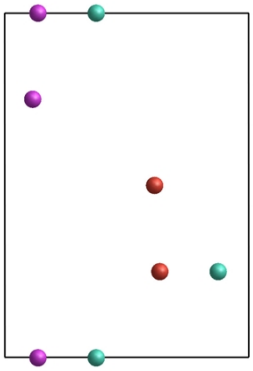

$cut2\delta_{h2}$

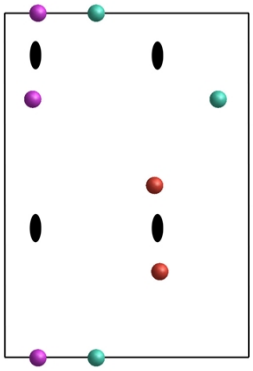

$cut2\delta_{h3}$

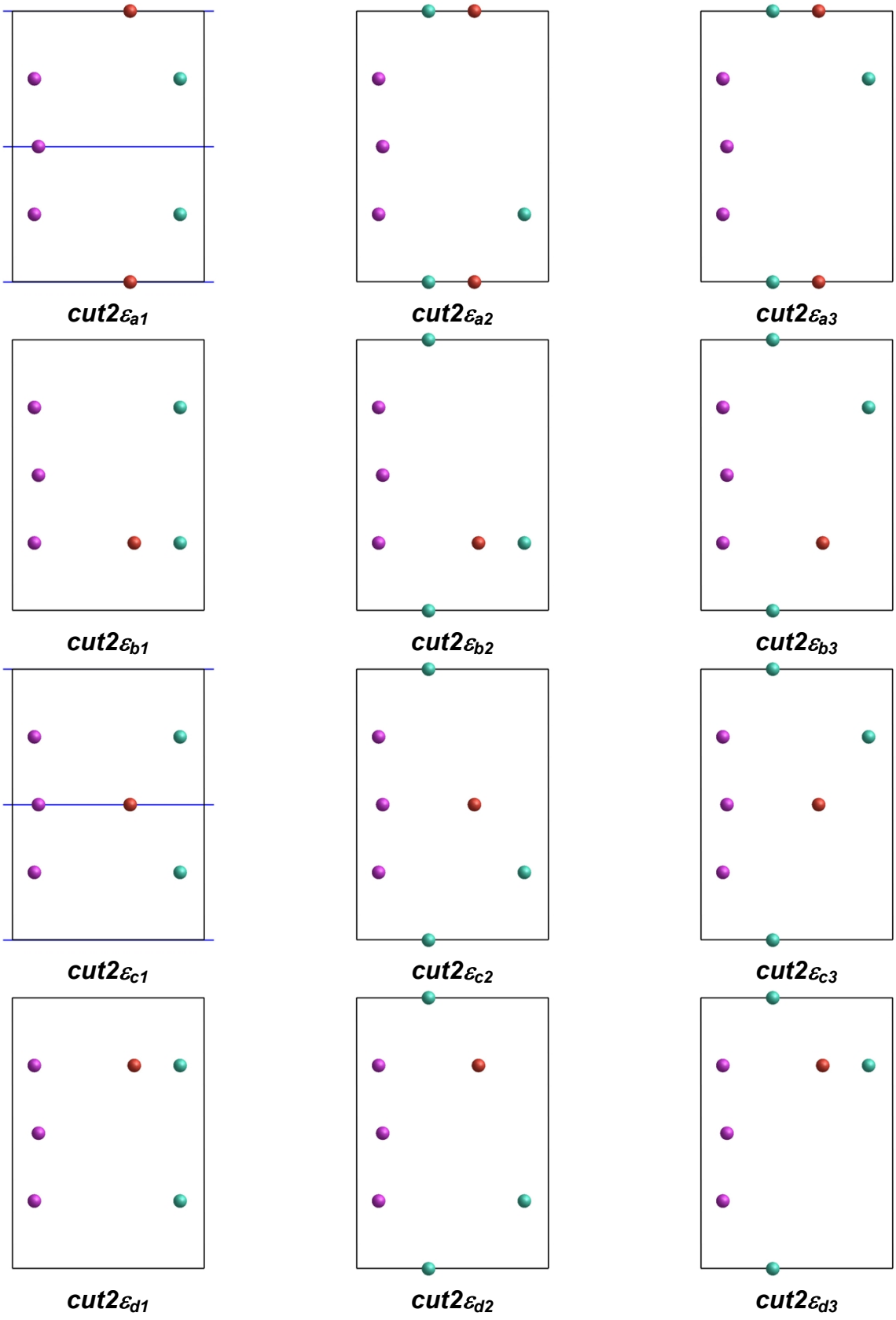

Figure S4. The fifty-four (110) cell configurations of the *cut2*. The colors stand: red for the O bonded to Mg (O1), purple for the O bonded only to Al (O2), greenish for the Al and blue for the Mg ions. The symmetry elements (the two-fold axes and the *m* planes) are reported as well.

Computational details (CRYSTAL09)

The *ab initio* CRYSTAL09 code[1,2] was employed, which implements the Hartree-Fock and Kohn-Sham self-consistent field (SCF) method for the study of periodic systems.[3] The crystal surfaces were simulated by using the 2D periodic slab model, consisting of a film formed by a set of atomic layers parallel to the *hkl* crystalline plane of interest.[4]

All the calculations were performed at the DFT (Density Functional Theory) level. In the Density Functional approach, the B3LYP Hamiltonian was adopted,[5-7] which contains a hybrid Hartree-Fock/Density-Functional exchange term and already shown to provide accurate results for structural and dynamical properties of garnet end members.[8]

In CRYSTAL the multi-electronic wave-function is constructed as an anti-symmetrized product (Slater determinant) of mono-electronic crystalline orbitals (COs) which are linear combinations of local functions (i.e.: atomic orbitals, AOs) centered on each atom of the crystal. In turn, AOs are linear combinations of Gaussian-type functions (GTF, the product of a Gaussian times a real solid spherical harmonic to give *s*-, *p*- and *d*-type AOs). In this study, two different Gaussian basis sets reproducing the multi-electronic wave-function were adopted: (i) BS1, where aluminum, oxygen, and magnesium were described by (8*s*)-(511*sp*)-(1*d*), (8*s*)−(411*sp*)−(1*d*), and (8*s*)−(511*sp*)−(1*d*) contractions, respectively;[9,10] (ii) BS2, with aluminum, oxygen, and magnesium described by (73211*s*)-(5111*p*)-(1*d*), (6211*s*)-(411*p*)-(1*d*) and (73211*s*)-(511*p*)-(1*d*) contractions, respectively.[11]

The thresholds controlling the accuracy in the evaluation of Coulomb and exchange integrals (ITOL1, ITOL2, ITOL3, ITOL4 and ITOL5, see Dovesi *et al.*[2]) were set to 10^{-8} (ITOL1 to ITOL4) and 10^{-16} (ITOL5). The threshold on the SCF energy was set to 10^{-8} Hartree.

In the adopted package the DFT exchange and correlation contributions are evaluated by numerically integrating functions of the electron density and of its gradient over the cell volume. The choice of the integration grid is based on an atomic partition method, originally developed by Becke.[12] In the present study, a *pruned* (75, 974) *p* grid was adopted (XLGRID in the code[2]), which ensured a satisfactory accuracy in the numerically integrated electron charge density (the error is on the order of $1 \cdot 10^{-4}$ |e| on a total of 1120 |e| for all the considered surfaces).

The reciprocal space was sampled according to a Monkhorst-Pack mesh[13] with shrinking factor 6, corresponding to 20 **k** points in the first irreducible Brillouin zone in both slabs e bulk, respectively.

Structures were optimized by using the analytical energy gradients with respect to atomic coordinates and lattice parameters within a quasi-Newton scheme, combined with the Broyden-Fletcher-Goldfarb-Shannon scheme for Hessian updating.[14-16] Convergence was checked on energy, gradient components and nuclear displacements. The threshold on energy between two subsequent

optimization steps was set to 10^{-7} Hartree; the thresholds on the root-mean-square of the gradient components and of the nuclear displacements were set to $3.0 \cdot 10^{-4}$ Hartree bohr^{-1} and $1.2 \cdot 10^{-3}$ bohr, respectively; those on the maximum components of the gradients and displacements were set to $4.5 \cdot 10^{-4}$ Hartree bohr^{-1} and $1.8 \cdot 10^{-3}$ bohr, respectively.

References

1 R. Dovesi, R. Orlando, B. Civalleri, C. Roetti, V.R. Saunders, C.M. Zicovich-Wilson, *Z. Kristallogr*, 2005, **220**, 571.
2 R. Dovesi *et al.*, *CRYSTAL09 User's Manual*; University of Torino: Torino, Italy, 2009.
3 C. Pisani, R. Dovesi, C. Roetti, *Hartree-Fock ab-initio treatment of crystalline systems*, Lecture Notes in Chemistry; Springer: Berlin, Heidelberg, New York, 1988.
4 R. Dovesi, B. Civalleri, R. Orlando, C. Roetti, V.R. Saunders, In: *Reviews in Computational Chemistry*; B.K. Lipkowitz, R. Larter, T.R. Cundari Eds.; John Wiley & Sons, Inc.: New York, 2005, vol.1, p.443.
5 A.D. Becke, *J. Chem. Phys.*, 1993, **98**, 5648.
6 C. Lee, W. Yang, R.G. Parr, *Phys. Rev. B* , 1998, **37**, 785.
7 P.J. Stephens, F.J. Devlin, C.F. Chabalowski, M.J. Frisch, *J. Phys. Chem.*, 1994, **98**, 11623.
8 R. Dovesi, M. De La Pierre, A.M. Ferrari, F. Pascale, L. Maschio, C.M. Zicovich-Wilson, *American Mineralogist*, 2011, **96**, 1787-1798.
9 Y. Noel, M. Catti, P. D'Arco, R. Dovesi, *Phys. Chem. Min.*, 2006, **33**, 383.
10 R. Demichelis, B. Civalleri, M. Ferrabone, R. Dovesi, *Int. J. Quantum Chem.*, 2010, **110**, 406.
11 M.F. Peintinger, D. Vilela Oliveira, T. Bredow, *J. Comput. Chem.*, 2013, **34**, 451.
12 A.D. Becke, *Phys. Rev. A*, 1998, **38**, 3098.
13 H.J. Monkhrost, J.D. Pack, *Phys. Rev. B*, 1976, **8**, 5188.
14 B. Civalleri, Ph. D'Arco, R. Orlando, V.R. Saunders, R. Dovesi, *Chem. Phys. Lett.*, 2001, **348**, 131.
15 K. Doll, *Comp. Phys. Commun.*, 2001, **137**, 74.
16 K. Doll, V.R. Saunders, N.M. Harrison, *Int. J. Quantum. Chem.*, 2001, **82**, 1.